Questa è la Dedica*:*
ognuno può scrivere quello che vuole,
anche nulla . . .

Contents

Introduction

Questa è l'introduzione.

Chapter 1

Neutrino Physics Overview

Questo è il primo capitolo.

1.1 Brief history

Neutrinos made their first appearence in modern physics as an hypothesized dark particle proposed by W. Pauli in order to solve the problem introduced by the continuous energy spectrum measured for β-decay electrons. Its name is though due to Enrico Fermi, the first scientist to take in serious consideration Pauli's hypothesis and develop a theory of beta decay that included the new particle as one of the four fermions involved in the corrisponded interaction. Fermi's theory led Bethe and Pearls to the first estimation of the inverse interaction's cross section:

$$\sigma(\bar{\nu}p \to ne^+) \leq 10^{-44}\ \mathrm{cm}^2, \quad E_{\bar{\nu}} \simeq 2\mathrm{MeV} \tag{1.1}$$

The smallness of the cross section led the two scientists to conclude thet it would be almost impossible to detect such an interaction.
Pontecorvo was the first to realize that by using a neutrino flux of about $10^{11}\nu/\mathrm{cm}^2/\mathrm{s}$, of the order of the one produced by an average nuclear reactor, and pointing it towards a ton mass scale detector one could obtain a rate of a few events per day. This idea was put into practice by Reines and Cowan, whose experiment led to the discovery of the anti-neutrino in 1956. Their technique for the identification of the $\bar{n}u$ relied on the detection of the light produced by the neutron, in delay with respect to the annihilation of the positron, a template still in use today.
In 1962 Lederman, Schwarts and Steinberger showed the existence of a second type of neutrino, associated with the muon in the main decay mode of the pion: $\pi^- \to \mu^-\bar{\nu_\mu}$. This was also the first case in which an accelerator

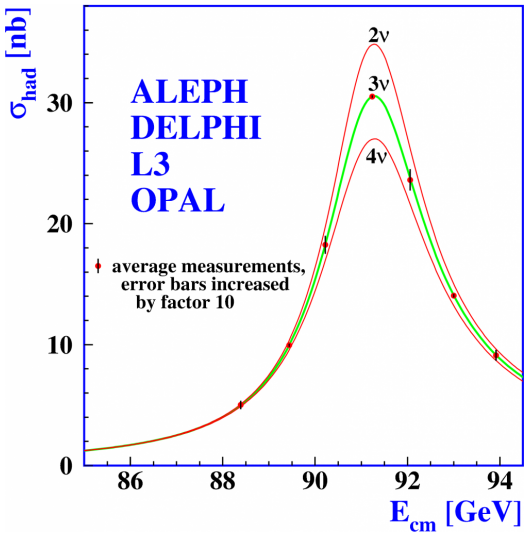

Figure 1.1: Theoretical predictions of the total cross-section for the production of hadrons as a function of the center of mass energy Ecm for 2, 3 and 4 neutrino families. Experimental data from LEP drawn as dots

neutrino beam was used in any experiment. Such beam was generated by the decay of pions and other adrons produced in the collision of accelerated protons on a thick shield. A neutrino detector was located behind, revealing the μ's produced in the ν_μ CC interactions.
During the seventies the accelerator at SLAC led to the discovery of the τ lepton, to which a third neutrino might be associated. The study of the decay width of the Z_0 produced at LEP in e^+e^- collisions excluded any number of SM neutrino families different from three (Fig. 1.1):

$$N_\nu = \frac{\Gamma_{inv}}{\Gamma_{\bar{\nu}\nu}} = 2.984 \pm 0.008 \tag{1.2}$$

The tau neutrino was finlly discovered at Fermilab in 2001 at the DONUT experiment by revealint the taus produced in CC interactions in iron.

1.2 Neutrinos in the Standard Model and neutrino masses

The Standard Model (SM) of particle physics is a gauge theory defined by the simmetry $SU(3) \times SU(2)_L \times U(1)_Y$ with the pedixes L and Y indicating the left chirality of the particles and their hypercharge respectively. The $SU(3)$ describes the quark interaction in the quark sector while $SU(2)_L \times$

$(1,2)_{-\frac{1}{2}}$	$(3,2)_{-\frac{1}{6}}$	$(1,1)_{-1}$	$(3,1)_{-\frac{2}{3}}$	$(3,1)_{-\frac{1}{3}}$
$\begin{pmatrix}\nu_e\\ e\end{pmatrix}_L$	$\begin{pmatrix}u\\ d\end{pmatrix}_L$	e_R	u_R	d_R
$\begin{pmatrix}\nu_\mu\\ \mu\end{pmatrix}_L$	$\begin{pmatrix}c\\ s\end{pmatrix}_L$	μ_R	c_R	s_R
$\begin{pmatrix}\nu_\tau\\ \tau\end{pmatrix}_L$	$\begin{pmatrix}t\\ b\end{pmatrix}_L$	τ_R	t_R	b_R

Table 1.1: All irreducible fermion rapresentations in the the SM, crouped according to their quantum numbers: $(d_{SU(3)}, d_{SU(2)})_Y$

$U(1)_Y$ is related to the electroweak sector.
The particles in the SM are divided into bosons of spin 1 that mediate the fundamental interactions (photons for the electromagnetic interactions, $W^\pm$ and Z^0 for the weak sector and 8 gluons for the strong sector), the spin 0 Higgs boson that together with the Higgs field is responsible for the Higgs mechanism and the fundamental fermions quarks and leptons, organized in $SU(2)_L$ left-handed doublets and $U(1)_Y$ right handed singlets (see Table).

Neutrinos are chargeless fermions that can interact only weakly, either via Neutral Current (NC) interactions mediated via Z^0 bosons or charged current via $W^\pm$ bosons. The flavour of the neutrino is simply defined by the charged lepton that is connected to the same charged current vertex:

$$\begin{aligned} W^+ &\to e^+ + \nu_e \\ &\to \mu^+ + \nu_\mu \\ &\to \tau^+ + \nu_\tau \end{aligned} \tag{1.3}$$

In this structure the weak interaction is parity violating and the neutrinos are either left-handed particles ν_L or right handed anti-particles $\bar{\nu}_R$. If neutrinos are Dirac fermions, this characteristic makes them massless in the Standard Model, since their mass term, written in its chiral components (Weyl spinors) would be given by :

$$\mathcal{L}_{mass}^{Dirac} = m_D(\bar{\psi}_L\psi_R + \bar{\psi}_R\psi_L), \text{ with } \bar{\psi}_R\psi_L = (\bar{\psi}_L\psi_R)^\dagger \tag{1.4}$$

It is obvious then that both a left and a right Dirac neutrino would have to exist for the mass term not to be null. This goes in contrast with the observation of neutrino flavour oscillations which, as we will discuss more in detail later (see Sec.), are possible only if the neutrinos are not massive

particles.
One strait away solution to this problem is to expand the Standard Model to include a right-handed neutrino ν_R so that the neutrino and its antiparticle can be described as a 4-state system in a Dirac spinor $\psi = (\psi_L, \psi_R)$, like all the other leptons. The fact that the neutrinos are neutral fermions though, opens up the possibility that they are in fact Majorana particles for which particle and antiparticle are two different spin states of the same particle.Such particles, theorized described by two states only. Such a fermion would be described by a single Weyl spinor. A Majorana mass term with a single Weyl-spinor, either left or right handed can be introduced as:

$$\mathcal{L}_{mass}^{Majorana} = -\frac{m_M}{2}[(\psi_L)^T i\sigma^2 \psi_L + h.c.]. \tag{1.5}$$

Such a mass term would violate the conservation of the fermionic "charges" by two units, making it plausible only for neutral particles. Since neutrinos have no known charges they can, in principle, both a Dirac and a Majorana term. This could be written as:

$$\mathcal{L}_{mass}^{\nu} = -\frac{1}{2}(\bar{\psi}_L, \bar{\psi}_L^c) \begin{pmatrix} m_{M,L} & m_D \\ m_D & m_{M,R} \end{pmatrix} \begin{pmatrix} \psi_R^c \\ \psi_R \end{pmatrix} \tag{1.6}$$

where c stands for the the conjugation operation.One can then do some considerations in order to simplify the mixing matrix. The Dirac mass term can be expected to be about the same as for the other fermions in the family and the mass term m_M, L should be small ($m_{M,L} \ll m_D$) since it can only be generated by a triplet of Higgs scalars, which is absent from the SM. Finally a right handed neutrino would be completely neutral under the standar-model gauge-group (i.e *sterile*), and it could have a mass above the symmetry breaking scale (v =246 GeV), without actually breaking any symmetry. The mass $m_{M,R}$ could then be associated to a different higher mass scale M. We then obtain the new matrix:

$$\mathcal{M} \simeq \begin{pmatrix} 0 & m_D \\ m_D & M \end{pmatrix} \tag{1.7}$$

This matrix can be diagonalized to obtain two eigenvalues that are approximatly M and $-m_D^2/M$. The two eigenvectors would then be two Majorana particles (per flavour), one very massive and sterile ($m_N \simeq M$) and one very light and weakly interacting ($m_\nu \simeq m_D^2/M$). The second particle would correspond to the neutrinos we normally observ. This so-called *see-saw* mechanism is largely considered to be one of the most natural of the possible explanations for the smallness of the neutrino masses.

The main experimental strategy used today if neutrinos are indeed Majorana particles or more canonical Dirac fermions is throgh the observation of the so called neutrinoless double beta decay, a process only possible if neutrinos and antineutrinos are the same particle. Some of the experiments now active in the field now include Gerda, CUORE and CuPID and CANDLES.

1.2.1 Limits on neutrino masses

While the existence of the neutrino oscillation phenomenon is an indicator of the fact that neutrinos must have a mass, as it will be discussed in Section, they depend only on the squared mass differences between different mass eigenstates and as such, they can't be used to obtain limits on the mass values. A direct measurement of neutrino masses is possible, in principle, using kinemathical methods, though these strategies have only produced upper limits so far.
For ν_e the most effective techinique relies on the measurement of the highest kinematically alowed energy in the β-decay spectrum. Such value is related to the neutrino mass as : $E^e_{\text{endpoint}} \simeq Q - m_\nu$. The best limit is currently set by the KATRIN experiment, which has recently halved the previous estimates from the Troitsk and Mainz experiments (all study the decay of tritium):

$$\begin{aligned} m_{\nu_e} &< 2.05 \text{ eV at } 95\% \text{ c.l. (Troitsk)}; \\ &< 2.3 \text{ eV at } 95\% \text{ c.l. (Mainz)}; \\ &< 1.1 \text{ eV at } 90\% \text{ c.l. (KATRIN)}; \end{aligned} \tag{1.8}$$

Limits on the masses of the other flavours are currently much less stringent and are obtained by studying the pion decay and the τ decay kinematics for ν_μ and ν_τ respectively:

$$\begin{aligned} m_{\nu_\mu} &< 170 \text{ keV at } 90\% \text{ c.l. }; \\ m_{\nu_\tau} &< 18.2 \text{ MeV at } 95\% \text{ c.l. }; \end{aligned} \tag{1.9}$$

Limits on the sum of the three masses can also be set by cosmological experiments such as WMAP. These limits are model dependent and in the Standard Cosmological Model are currently set at:

$$\sum_j m_j \leq 0.3 - 1.3 \text{ eV} \tag{1.10}$$

Finally the non observation of double beta decay can set a limit on the electron neutrino effective mass in the case that neutrinos are Majorana particles:

$$\langle m_{\nu_e} \rangle_{eff} \lesssim 0.4 \text{ eV} \tag{1.11}$$

1.3 Theory of Neutrino Oscillations

If neutrinos have non-vanishing rest mass, the weak and mass eigenstates are not necesserily the same, a fact that is well known in the quark sector where the CKM matrix connects the two types of states. This makes the phenomenon of neutrino oscillations possible i.e. a neutrino produced with a specific flavour can later be measured to have a different flavour. The experimental discovery of this new behaviour in 1998 is today the strongest evidence of the fact that the neutrinos have mass and one of the most powerfull probe into their properties.

1.3.1 Three flavors oscillations in vacuo

We start by considering the case where we have 3 orthonormal flavor eigenstates $|\nu_\alpha\rangle$ (where $\alpha = e, \mu, \tau$)which are connected to 3 orthonormal mass eigenstates $|\nu_i\rangle$ via a unitary mixing matrix U:

$$|\nu_\alpha\rangle = \sum_i U_{\alpha i} |\nu_i\rangle \ ; \quad |\nu_i\rangle = \sum_\alpha U^*_{\alpha i} |\nu_\alpha\rangle \ ; \tag{1.12}$$

The unitary U matrix, in the case of 3 neutrino flavor and mass eigenstats is the so called PMNS (Pontecorvo-Maki-Nakagawa-Sakata) matrix and can be written as:

$$\begin{aligned} U &= \begin{bmatrix} 1 & 0 & 0 \\ 0 & c_{23} & s_{23} \\ 0 & -s_{23} & c_{23} \end{bmatrix} \quad \begin{bmatrix} c_{13} & 0 & s_{13}e^{-i\delta} \\ 0 & 1 & 0 \\ -s_{13}e^{i\delta} & 0 & c_{13} \end{bmatrix} \quad \begin{bmatrix} c_{12} & s_{12} & 0 \\ -s_{12} & c_{12} & 0 \\ 0 & 0 & 1 \end{bmatrix} = \\ &= \begin{bmatrix} c_{12}c_{13} & s_{12}c_{13} & s_{13}e^{-i\delta} \\ -s_{12} - c_{12}s_{23}s_{13}e^{i\delta} & c_{12}c_{23} - s_{12}s_{23}s_{13}e^{i\delta} & s_{23}c_{13} \\ s_{12}s23 - c_{12}c_{23}s_{13}e^{i\delta} & -c_{12}s_{23} - s_{12}c23s_{13}e^{i\delta} & c_{23}c_{13} \end{bmatrix} \end{aligned} \tag{1.13}$$

where $c_{ij} = \cos\theta_{ij}$, $s_{ij} = \sin\theta_{ij}$, θ_{ij} are the mixing angles and δ is the Dirac CP violating phase. In the case of Majorana neutrinos the matrix contains two addictional Majorana phases which appear in a diagonal matrix that multiplies U:

$$U^{Majorana}_{\alpha 1} = U_{\alpha i} e^{\lambda_k} \tag{1.14}$$

These additional phases do not affect neutrino oscillations and cannot be measured in neutrino oscillation experiments, while all the other parameers entering te matrix can be.

The mass eigenstates $|\nu_i\rangle$, being the eigenstates of the Hamiltonian ($\mathcal{H}|\nu_i\rangle = E_i|\nu_i\rangle$) show a time dependence :

$$|\nu_i(t)\rangle = e^{-iE_it}|\nu_i\rangle \tag{1.15}$$

with $E_i = \sqrt{\vec{p}^{\,2} + m_i^2}$ being the eigenvalues. If we now consider a flavor state $|\nu_\alpha(t)\rangle$ which represents a neutrino of definite flavour created at t=0, from eq. 1.12 and 1.15 the time evolution of this state is given by:

$$\begin{aligned} |\nu_\alpha(t)\rangle &= \sum_i U_{\alpha i} e^{-iE_it}|\nu_k\rangle \\ &= \sum_\beta \Big(\sum_i U^*_{\alpha i} e^{-iE_it} U_{\beta i}\Big)|\nu_\beta\rangle \end{aligned} \tag{1.16}$$

The superposition of massive neutrino states, which is a pure flavor state at t=0 ($|\nu_\alpha(t=0)\rangle = |\nu_\alpha\rangle$), becomes a superposition of different flavor states at $t > 0$. The amplitude of the transition of $\nu_\alpha \to \nu_\beta$ as a function of time is then:

$$\mathcal{A}_{\nu_\alpha\to\nu_\beta}(t) = \langle\nu_\beta|\nu_\alpha(t)\rangle = \sum_i U^*_{\alpha i} U_{\beta k} e^{-iE_it} \tag{1.17}$$

The transition probability is given by the square of the amplitude:

$$P_{\nu_\alpha\to\nu_\beta}(t) = |\mathcal{A}_{\nu_\alpha\to\nu_\beta}(t)|^2 = \sum_{i,j} U^*_{\alpha i} U_{\beta i} U_{\alpha j} U^*_{\beta j} e^{-i(E_i-E_j)t} \tag{1.18}$$

In the case that the neutrinos are ultrarelativistic ($v \sim c$) we can approximate:

$$E_i \simeq E + \frac{m_i^2}{2E}; \qquad t \simeq L; \tag{1.19}$$

with L being the distance between the source and the detector. The probbility then becomes:

$$P_{\nu_\alpha\to\nu_\beta}(L,E) = \sum_{i,j} U^*_{\alpha i} U_{\beta i} U_{\alpha j} U^*_{\beta j} \exp\left(-i\frac{\Delta m^2_{ij} L}{2E}\right) \tag{1.20}$$

The oscilation probability is then dependent on a set of natural parameters, namely the square difference between the mass eigenstates $\Delta m^2_{ij} = m_i^2 - m_j^2$, the three mixing angles θ_{ij} and the Dirac CP violation phase δ. It also depends on the L/E ratio, which is one of the main features defining the different types of neutrino oscilation experiments (see Sec). It does not however, depend on the absolute mass values of the eigenstates, making it impossible to detemine them in neutrino oscillation experiments. These experiments

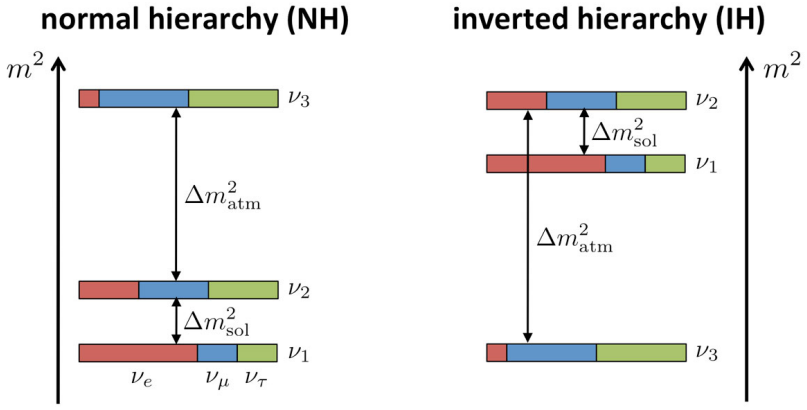

Figure 1.2: Neutrino mass eigenstates possible orderings in normal (left) and inverted (right) hierarchy. The flavor composition of the three states is shown by dividing the bars into colors: red for $\nu_e$blue for ν_μ and green for ν_τ.

also do not provide any information about the sign of the square mass differences and are only sensitive to Δm^2_{23} and Δm^2_{13} which are also commonly referred to as *atmosferic* and *solar* mas differences, depending on the type of experiment (Sec). Two scenarios consistent with the experimental measurements are then possibile: the so-called *normal* and *inverted hierarchy*. In normal hierarchy, neutrino mass eigenstates are ordered $m_1 < m_2 < m_3$, while in inverted hierarchy $m_3 < m_1 < m_2$ (Fig. 1.2).

1.3.2 CP violation

Knowing from experimental results that all mixing angles are not null, especially θ_{13}, we can see from the mixing matrix, that if the Dirac phase δ is not null, it can generate CP violation effects in neutrino oscillation. CP violation is manifested if the oscillation probability of $\nu_\alpha \to \nu_\beta$ are different from the CP conjugate $\bar{\nu}_\alpha \to \bar{\nu}_\beta$. An observable for such effects would then be the probability asimmetry:

$$\mathcal{A}^{CP}_{\alpha\beta} = P(\nu_\alpha \to \nu_\beta) - P(\bar{\nu}_\alpha \to \bar{\nu}_\beta); \quad \alpha \neq \beta \text{ and } \alpha, \beta = e, \nu, \tau \tag{1.21}$$

As a consequence of the CPT theorem a CP asymmetry would imply a T asymmetry offering a second observable:

$$\mathcal{A}^{T}_{\alpha\beta} = P(\nu_\alpha \to \nu_\beta) - P(\nu_\beta \to \nu_\alpha); \quad \alpha \neq \beta \text{ and } \alpha, \beta = e, \nu, \tau \tag{1.22}$$

In the three neutrino mixing case the magnitude of the CP violation is determined by the so-called Jarlskog invariant $J^{CP}_{\alpha\beta}$ in direct analogy with the quark sector:

$$\mathcal{A}^{CP}_{\alpha\beta} = -16 J^{CP}_{\alpha\beta} \sin\left(\frac{\Delta m^2_{12}}{4E}L\right) \sin\left(\frac{\Delta m^2_{23}}{4E}L\right) \sin\left(\frac{\Delta m^2_{13}}{4E}L\right) \quad \text{with } J^{C}_{\alpha\beta}P = Im[U_{\alpha 1}U^*_{\alpha 2}U^*_{\beta 1}U_{\beta 2}] = \pm c_{12}s_{12}c_{23}s_{23}c^2_{13}s_{13}\sin\delta \tag{1.23}$$

using the same notation as in . The size of CP violation in the neutrino sector is still unknown since the Dirac phase δ in still unknown. Current data for the mixing angles inply that the value of $J^{CP}_{\alpha\beta}$ should be in the range of:

$$0.026|\sin\delta| \lessapprox |J^{CP}_{\alpha\beta}| \lessapprox 0.036|\sin\delta| \tag{1.24}$$

For CP violation effects to be observable both $\sin(\frac{\Delta m^2_{31}L}{2E})$ and $\sin(\frac{\Delta m^2_{21}L}{2E})$ should be large. This is why most future and present experiment that want to perform such measurements are long baseline experiments with ν_μ and $\bar{\nu}_\mu$ accelerator beams with energy from $0.7GeV$ up to a few GeV.

1.3.3 Two flavor scenario

An important approximation of the neutrino oscillation phenomenon is the special case in which only two flavours are considered. This casistic is not didactical since it is simpler then the 3-flavour case, but is also usefull in data analysis since most experiments are sensible only to the oscillations between two neutrino flavours.
In this simplified case therelation between the neutrino states is described by one mixing angle and one mass dfference. The unitary trasformation then becomes a two-dimensional rotation, analogus to the Cabibbo matrix in the quark sector. In the cas of ν_e and ν_μ we get:

$$\begin{pmatrix}\nu_e\\ \nu_\mu\end{pmatrix} = \begin{pmatrix}\cos\theta & \sin\theta\\ -\sin\theta & \cos\theta\end{pmatrix}\begin{pmatrix}\nu_1\\ \nu_2\end{pmatrix} \tag{1.25}$$

The two-flavor transition probability ,using the formulas fromthe previous secion then becomes:

$$P(\nu_e \to \nu_\mu) = \sin^2 2\theta \times \sin^2\left(\frac{\Delta m^2 L}{4E}\right) \tag{1.26}$$

Since no CP violating phase is present his is the same for $P(\nu_\mu \to \nu_e)$ and for $P(\bar{\nu}_e \to \bar{\nu}_\mu)$.

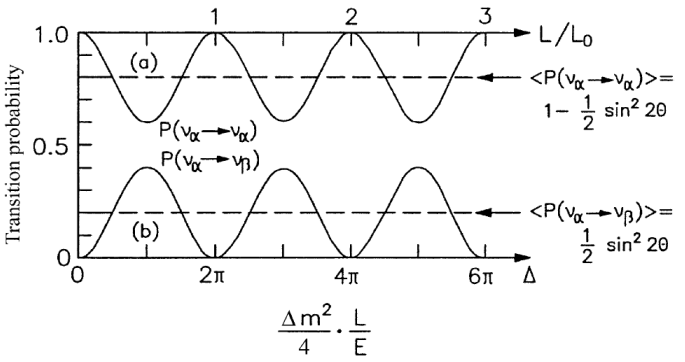

Figure 1.3: Two flavor oscillation probability as a functionof L/L_0 :disappearene $P(\nu_\alpha \to \nu_\alpha)$ (up);appearence $P(\nu_\alpha \to \nu_\beta)$

The *survival* probability of the particle not changing flavor is simply .

$$P(\nu_e \to \nu_e) = 1 - P(\nu_e \to \nu_\mu) \tag{1.27}$$

The oscillatory term can also be rewritten as:

$$\sin^2\left(\frac{\Delta m^2 L}{4E}\right) = \sin^2\left(\pi \frac{L}{L_0}\right) \qquad \text{with } L_0 = 4\pi\hbar c \frac{E}{\Delta m^2} \tag{1.28}$$

where L_0 is the oscillation length and describes the period of one full oscillation cycle. It is proportional to E, and inversely proportional to Δm^2. The oscillation probability will then be maximum for $L/L_0 = 1/2$ and its amplitude will be given by $\sin^2\theta$ (Fig. 1.3).

1.3.4 MSW Matter Effects

When neutrinos travel though dense matter, their propagation can be modified by the coherent forward scattering they experience from particles along their trajectories. The oscillation probability can then become rather different then in vacuum as it was first noticed by Mikhaev, Smirnov and Wolfenstein (MSW), from which the effect takes its name.
The MSW effect has origin from the fact that ν_e and $\bar{\nu}_e$ are the only neutrino flavor that can take part both in charged current interactions, and NC elastic interactions with electrons, while ν_μ and ν_τ can only have NC interactions with electrons. This introduces and extra potential :

$$V_e = \pm\sqrt{2} G_F N_e \tag{1.29}$$

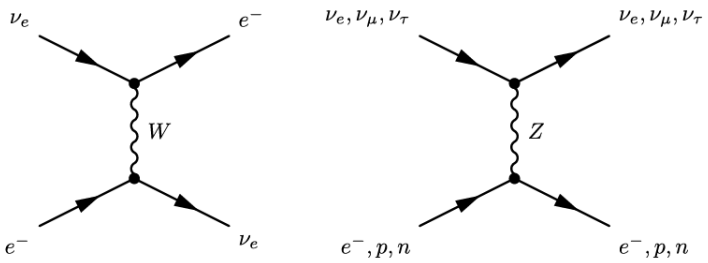

Figure 1.4: Feynmann diagram of CC electronic neutrino interactions $\nu_e + e^- \to \nu_e + e^-$ (left) and of NC neutrino interactions $\nu_\alpha + e^- \to \nu_\alpha + e^-$ (right)

where N_e is the electron density in the medium, G_F is the Fermi constant and the sign is positive for neutrinos and negative for antineutrinos.

Using a simplified two flavor approach the effective Hamiltonian of neutrino propagation in matter then gains an extra $\nu_e - \nu_e$ element and becomes:

$$\mathcal{H}_M = \mathcal{H} + \begin{pmatrix} V_e & 0 \\ 0 & 0 \end{pmatrix} = \left(\frac{\Delta m^2}{4E}\right) \begin{pmatrix} -\cos 2\theta & \sin 2\theta \\ \sin 2\theta & \cos 2\theta \end{pmatrix} + \begin{pmatrix} V_e & 0 \\ 0 & 0 \end{pmatrix} \tag{1.30}$$

In the simple case where the matter density is constant, we can then rediagonalise $\mathcal{H}_M$ to obtain a new mixing matrix and mass eigenstates. We can then denote the new effective parameters as θ_M and Δm^2_M and the oscillation probability takes the usual form:

$$P(\nu_e \to \nu_\mu) = \sin^2 2\theta_M \sin^2\left(\frac{\Delta m^2_M L}{4E}\right) \tag{1.31}$$

The new parameters can be obtain from eq and are:

$$\begin{aligned} \Delta m^2_M &= M \Delta m^2 \\ \sin 2\theta_m &= \frac{\sin 2\theta}{M} \end{aligned} \tag{1.32}$$

with coefficient M being:

$$M = \sqrt{\left(\cos 2\theta - \hat{A}\right)^2 + \sin^2 2\theta} \tag{1.33}$$

with:

$$\hat{A} = \pm \frac{2\sqrt{2} G_F N_e E}{\Delta m^2} \tag{1.34}$$

Matter effects have somery crutial consequenses in the field of neutrino oscillation:

1. Either long travel ditances or high matter densities are necessary in order for the MSW effects to be appreciable (if $\Delta m^2_M L/4E << 1$ we return to vacuum probabilities)

2. There is a resonant condition for which the oscillation probability is significantly enhanced with respect to the one in vacuum. That is when:
$$\hat{A} = \cos 2\theta \tag{1.35}$$

3. Oscillation probabilities can be different for neutrinos and antineutrinos even if there are is no CP violation, due to the $\pm$ sign in the effective potential V_e.

4. The resonant condition can be met only if $\hat{A} > 0$, which depends on the sign on the sign of the square mass difference Δm^2. This fact makes matter effects an effective probe to study mass hierarchy. In particular it can be studied in long baseline accelerator experiments which are sensitive to electron-muon neutrino oscillation ($\Delta m^2 \sim \Delta m^2_{23}$) if L and E are high enough.

1.4 Neutrino oscillation experiments

The first subdivision between different neutrino oscillation experiments is determined by what the experiment is trying to measure:

- **Appearence experiments**: These experiments look for signals from neutrino flavours that are not present in the initial composition of the flux. The background can be rather small for these experiments, which make them sensitive to small mixing angles.

- **Disappearence experiments**: These experiments measure the number of signals from the various flavours of neutrinos and confront it with the expected one in order to compute the survival probability.

The second distinction is then between the different sources of neutrinos then can be used. The most important ones are:

- **Reactor experiments**: they use large fluxes of $\bar{\nu}_e$ produced by beta decays of fission fragments in nuclear power plants;

- **Accelerator experiments**: they use beams of neutrinos produced in decays of secondary mesons (mainly π and K) or muons, generated by a proton beam hitting a target. These can be further devided depending

on how the beam is produce. Firstly we have"**Pion decay in flight**" or **DIF** beams which are at higher energies and are mailnly composed of either ν_μ or $\bar{\nu}_\mu$ depending on the polarity of the horn focalizing the mesons, with a small percentage of ν_e from tertiary muon decay. Secondly we have "**Muon decay at rest**" or **DAR** which are in a lower energy range. Finally there are the so called **Beam dump** or **prompt** neutrino experiments, in which the proton beam is at very high energy (hundreds of GeVs) and is completely "dumped" in a thick target generating heavy hadrons which equally decy in electron and proton neutrinos;

- **Atmospheric neutrino experiments**: they detect atmospheric neutrinos produced in the atmospheric cosmic ray showers;

- **Solar neutrino experiments**: they detect neutrinos generated in thermonuclear reactions in center of the Sun;

This distinction is important not only because of the very different experimental setups, but also because the neutrino source and where the detectors are located with respect to it, determine the consts of nature to which the experiments are sensitive. Specifically experiments can be sorted according to the value of Δm^2 to which they are sensitive. The condition for an experiment to be sensitive to a specific mass squared difference is that:

$$\frac{\Delta m^2 L}{2E} \sim 1 \tag{1.36}$$

If this value is too small the oscillation simply does not occur, if it is too large only the average transition probability is measurable and no information on Δm^2 can be obtained. The different experiments are then classified depending on the ratio L/E, which determines the sensitivity:

- **Short BaseLine (SBL)**: These are either reactor or accelerator experiments. In the first case the experiments measure the survival probability and and are active in the L/E range:

$$\frac{L}{E} \lesssim 10\text{m/MeV} \implies \Delta m^2 \gtrsim 1\text{eV}^2 \tag{1.37}$$

  In the case of accelerator experiments the range varies depending on

the type of beam:

$$\begin{aligned} \frac{L}{E} &\lesssim 1\text{km/GeV} \quad \Longrightarrow \quad \Delta m^2 \gtrsim 1\text{eV}^2 \ (DIF) \\ \frac{L}{E} &\lesssim 1\text{m/MeV} \quad \Longrightarrow \quad \Delta m^2 \gtrsim 1\text{eV}^2 \ (DAR) \\ \frac{L}{E} &\lesssim 10^{-2}\text{m/MeV} \quad \Longrightarrow \quad \Delta m^2 \gtrsim 10^2\text{eV}^2 \ (Beam\ dump) \end{aligned} \tag{1.38}$$

- **Long BaseLine (LBN)**: these experiments have sources similar to SBL ones but have a distance between source and detector that is 10 or 100 times larger:

$$\begin{aligned} \frac{L}{E} &\lesssim 10^3\text{km/GeV} \quad \Longrightarrow \quad \Delta m^2 \gtrsim 1\text{eV}^2 \ (Accelerator) \\ \frac{L}{E} &\lesssim 10^3\text{m/MeV} \quad \Longrightarrow \quad \Delta m^2 \gtrsim 1\text{eV}^2 \ (Reactor) \end{aligned} \tag{1.39}$$

  In this cathegory are also included the Atmospheric neutrino experiments:

$$\frac{L}{E} \lesssim 10^4\text{km/GeV} \quad \Longrightarrow \quad \Delta m^2 \gtrsim 1\text{eV}^2 \ (ATM) \tag{1.40}$$

- **Very Long BaseLine (VLB)**: these experiments have a distance between source and detector that is 10 or 100 times larger then for LBN experiments:

$$\begin{aligned} \frac{L}{E} &\lesssim 10^5\text{m/MeV} \quad \Longrightarrow \quad \Delta m^2 \gtrsim 10^{-5}\text{eV}^2 \ (Reactor) \\ \frac{L}{E} &\lesssim 10^4\text{km/GeV} \quad \Longrightarrow \quad \Delta m^2 \gtrsim 10^{-4}\text{eV}^2 \ (Accelerator) \end{aligned} \tag{1.41}$$

  In this cathegory are also included the Solar neutrino experiments:

$$\frac{L}{E} \lesssim 10^{12}\text{m/MeV} \quad \Longrightarrow \quad \Delta m^2 \gtrsim 10^{-12}\text{eV}^2 \ (Sol) \tag{1.42}$$

1.4.1 Solar experiments: θ_{12} and Δm^2_{12}

The Sun produces an intense flux of neutrinos as a subproduct of some of the thermonuclear reactions that produce energy in its interior by burning hydrogen into helium. There are two main cycles of reactions that can produce neutrinos : the pp cycle and CNO (Carbon-Nytrogen-Oxygen) cycle. Both can be summarized as:

$$4p \rightarrow \ ^4He + 2e^- + 2\nu_e \tag{1.43}$$

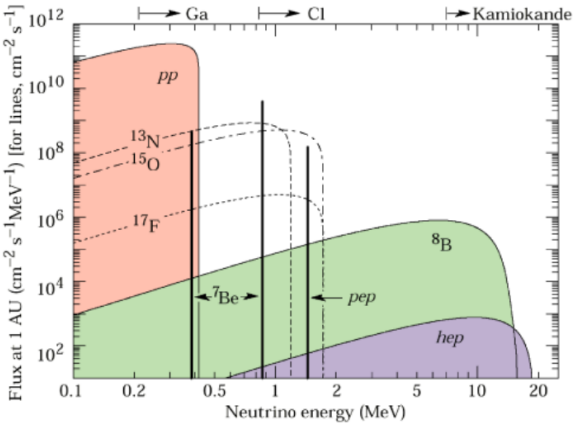

Figure 1.5: Spectrum of solar neutrinos, modelled from the SSM. The arrows indicate the sensitivity range of some of the experiments

The expected flux of electron neutrinos, in the hypothesys that they are massless can be computed using the standard solar model (SSM), which is a detailed simulation of the reactions taking place in the solar interior.
The solar neutrino experiments can be devided into two main cathegories depending on the revelation techniques: radiochemical and Cherenkov. In the first field we find experiments such as Homestake, Gallex/GNO and Sage (using ^{3}7Cl, ^{7}1Ga and 71Ge respectively). These have a relatively low energy threshold ($E_\nu \gtrsim 0.23 - 0.81$ MeV) for all flavours of neutrinos, but they are not able to give any information on direction, energy or time of the event.
The Cherenkov technique was pioneered by the Kamiokande experiment, consisting of a tank of about 3000 tons of pure water and 1000 photomultipliers positioned on the inner walls. It consisted in observing the Cherenkov light produced by recoil electrons in elastic scattering interactions of ν_e with e^-, which have a larger threashold of $E \gtrsim 5$MeV:

$$\text{(ES)} \quad \nu_e + e^- \to \nu_e + e^- \qquad E \gtrsim 5\text{MeV} \tag{1.44}$$

This technique was capable of measuring neutrino interactions in real time while also giving informations on direction and energy. This capability was crutial in conferming the existence of the so called *solar neutrino problem*, a deficit in the number of neutrinos arriving from the Sun between 1/2 and 2/3 with respects to the predictions of the SSM, measured by the earlier radiochemical experiments.
The Kamiokande experiment was not able to measure both the flux of ν_e and the combined flux between the three flavors. This was made possible by the SNO experiment in which, thanks to the use of heavy water (d_2O)

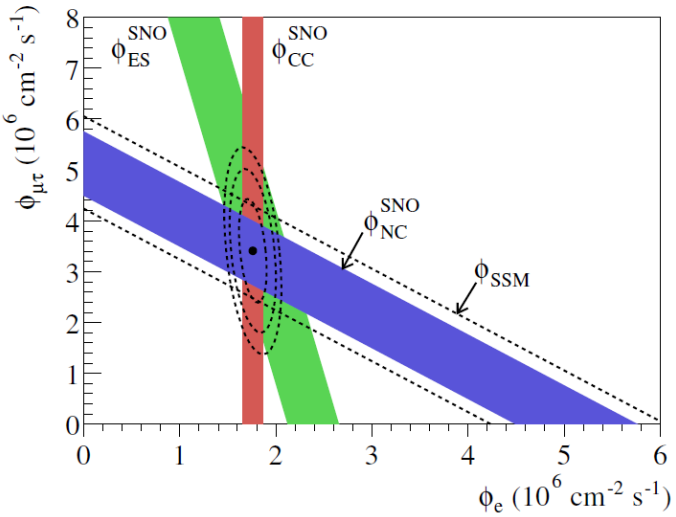

Figure 1.6: Flux of muon and tau neutrinos $\phi_{\mu\tau}$ over electron neutrino ϕ_e as measured by SNO. The three colored bands correspond to the three possible interactions: electron scattering ES (green); charged current CC (red); neutral current NC (blue). The dashed band gives the prediction from the SSM which is in agreement with the NC measurements.

rather than purified water as target, two more reactions were available for detection:

$$\begin{aligned} &\text{(CC)} \quad \nu_e + d \to p + p + e^- ; \quad E \gtrsim 5\text{MeV} \\ &\text{(NC)} \quad \nu_f + d \to p + n + \nu_f ; \quad f = e, \mu, \tau \quad E \gtrsim 2.2\text{MeV} \end{aligned} \tag{1.45}$$

Since the first reaction is sensitive only to ν_e while the second is sensitive to all flavors, one can compare the two rates in order to establish if the solar neutrino flux contains ν_μ and ν_τ or not and in which measure. What SNO found was that the combined tau and mu fluxes were two times more intense than the ν_e one and that the total flux was in agreement with the predictions from the SSM (Fig. 1.6).
The results from solar neutrino experiments can be interpreted as due to flavor oscillation. The characteristic L/E for these experiments are of the VLB range, making them sensitive to the Δm^2_{12} mass squared difference and to $\sin 2\theta_{12}$. For this reason the two parameters are often referred to as solar mass difference and solar mixing angle $(\Delta m^2_\odot, \theta_\odot)$. As already noted these two parameters can be measured also by VLB reactor experiments such as KamLand (discussed in Section). The most precise values for the paramenters are obtained combining the results from both (Fig. 1.7).
Other important and more recent Solar experiments include Borexino, which

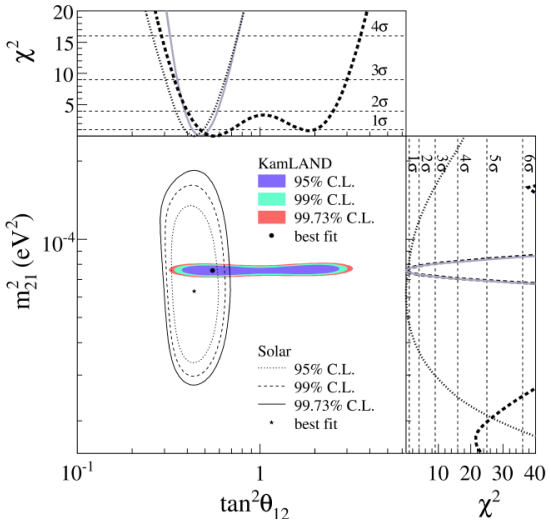

Figure 1.7: Confidence level intervals for the solar oscillation parameters from KamLAND and the combined results from solar experiments. The side-panels show the respective χ^2 profiles: KamLAND (dashed); solar experiments (dotted) individually; combined (solid)

was the first with an energy threashold low enough to measure the monochromatic flux of ^7Be and *pep* neutrinos and Super-K, the successor of Kamiokande. The results from both experiments are in agreement with the neutrino oscillation hypothesys.

1.4.2 Reactor experiments

VLB: confermation of solar experiment results

Neutrinos from nuclear reactors are mostly $\bar{\nu}_e$ with energy of the order of the MeV. This makes the particles above threshold for electronic CC interactions, but not for other flavors, which means that if the neutrino oscillates it cannot be detected anymore. Reactor experiments can then measure the disappearence probability of the $\bar{\nu}_e$ and they are usually sensitive to small values of Δm^2 due to the low energy spectrum of the neutrinos.
Very Long Baseline experiments proved to be sensitive to the solar square mass difference and were able to give confermation on the Solar experiment results, while at the same time improving the sensitivity to the parameter and beginning the precision era of neutrino physics.
In particular the KamLAND experiment, located in the Kamioka mines in Japan , was the first to give independent confermation of the results from

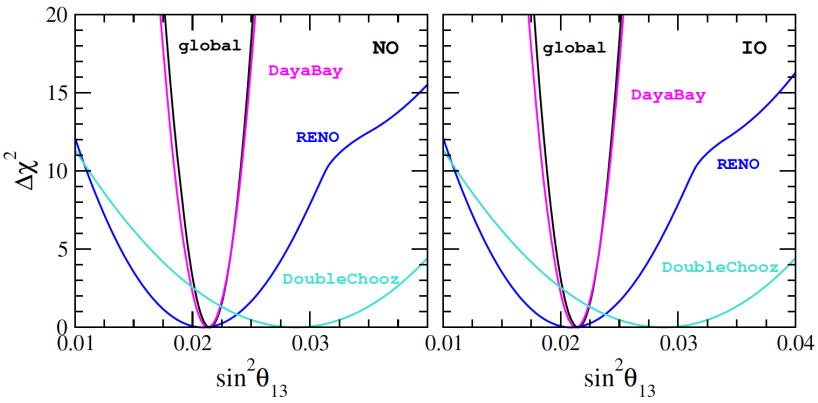

Figure 1.8: χ^2 profile as a function of $\sin\theta_{13}$ for RENO DataBay and Double Chooz and the combined result (black line). The results are fitted for normal ordering (left) and inverse ordering (right)

the solar neutrino sector. It consists of a 1000 ton liquid scintillator detector measuring the interactions of $\bar{\nu}_e$ from a cluster of nuclear reactors located at an average distance of $L \simeq 175$km. The antineutrinos interact via inverse beta decay at an energy theashold of $E > 2.6$MeV:

$$\bar{\nu}_e + p \rightarrow e^+ + n \qquad E > 2.7 \text{ MeV} \tag{1.46}$$

As mentioned in Section, this is the same reaction used by Reines and Cowan in their famous experiment and the signature given by the e^+ annihilation and the delayed neutron thermalization and capture proved very effective in the reduction of background. This level of precision was also crutial in excluding alternative explanations for neutrino oscillations based on exotic interactions or magnetic transition moments.

Measurement of θ_{13}

Recently Long Baseline experiments such as Daya Bay, RENO and Double Chooz have been able to measure the disappearence of reactor electron antineutrinos at distances $L \sim 1$ km. This is the typical L/E for which oscillations are mainly driven by the mixing angle θ_{13}.
Compared to previous experiments such as CHOOZ and Paloverde, these have not only access to larger statistics, thanks to the increased reactor power and larger detectors,but they also have access to multiple detectors at different distances from the reactor core. Measurements at the closest detectors can then be utilized to more accuratly predict the expected number of

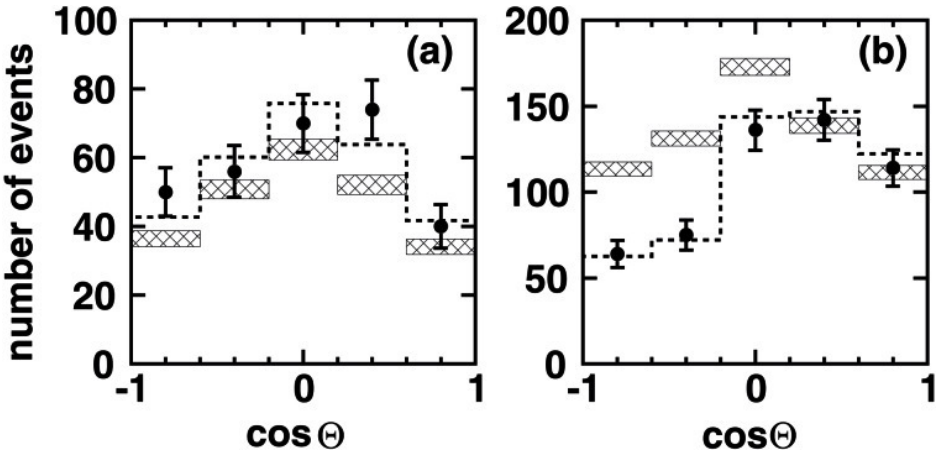

Figure 1.9: Zenith angle Θ distributions for the most energetic multi-GeV atmospheric neutrino events measured by Super-Kamiokande over a 535 days period. Coloured histograms are the Monte Carlo predictions and dotted histograms are the experimental measurements. Right and left panels are μ-like and e-like events respectively.

events at the more distant ones.
The combined results from the experiments are shown in Fig. 1.8

1.4.3 Atmospheric experiments: Δm^2_{31} and θ_{23}

The cosmic ray interactions with the atmospher nitrogen and oxygen nuclei produce mostly pion and kaons that decay in electron and muon neutrino as well as antineutrinos. ν_e decay from the chain : $\pi \to \mu\nu_\mu$ followed by $\mu \to e\nu_\mu\nu_e$. One then would expect the ratio to be of the order:

$$R = \frac{N(\nu_\mu + \bar{\nu_\mu})}{N(\nu_e + \bar{\nu_2})} \sim 2 \tag{1.47}$$

Experiments originally built to look for proton decay in the '70s and '80s, which had atmospheric neutrinos as background, were the first to observe a deficit with respect to the Monte Carlo expectations, measured originally as the ratio : $R_{\mu/e}/R^{MC}_{\mu/e}$. Two main cathegories of detectors were in operation: water Cherenkov tanks such as Super Kamiokande and iron calorimeters such as Soudan2 and Macro. The first kind of detectors are constituted of tanks filled with water in the order of 1 ton, and they detect the Cherenkov light rings produced by the charged lepton using photo multipliers placed on the inside of the walls. Iron calorimeters are instead constituted of layers of iron, acting as a passive materials and active layers, made for example of plastic

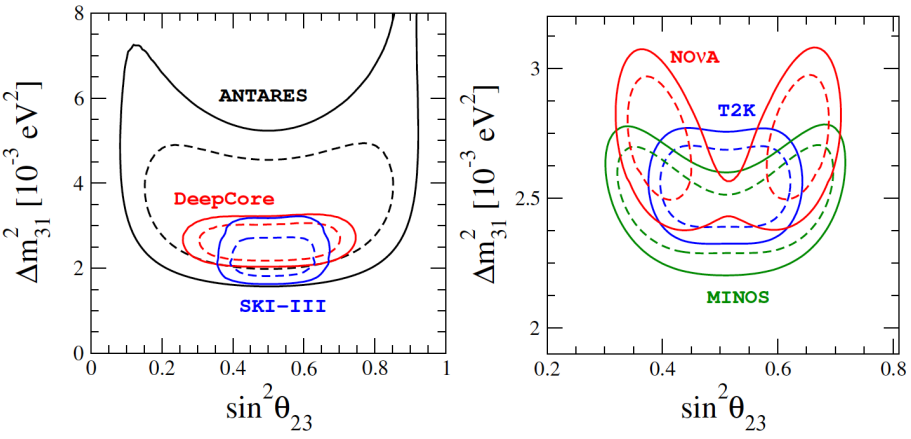

Figure 1.10: 90% CL (straight line) and 99% CL(dashed line) C.L. regions in the atmosferic parameter plane (Δm^2_{31} over $sin^2\theta_{23}$ from atmospheric (left) and long baseline accelerator (right) experiments, assuming normal mass hierarchy.

drift tubes, which track either the electromagnetic showers produced by $e^{\pm}$ or long muonic tracks. Both techniques are capable of flavour identification and direction and energy estimation.
In 1998 the SuperKamiokande identified the origin of this anomaly to be caused by neutrino oscillation. The experiment distinguished between muon and eletron neutrino events, measured the lepton zenith angle with respect to the Earth's axis (correlated to that of the parent neutrino) and divided the samples differantiating between the lepton energy (the more energetic events having a stronger direction dependency with that of the parent neutrino). These measurements made it possible to observe the variation of the flux as a function of the energy and zenith angle and thus the L/E travelled by the parent neutrino (Fig.1.9).
SuperK showed that while the electron events had no observed reduction, the muon events had a deficit of almost 50% for up-going neutrinos ($\cos\Theta = -1$). This is explained considering a flavour oscillation dominated by the parameters $\Delta m^2_{23} \sim \Delta m^2_{13}$ and θ_{23} that for this reason are often referred to as atmospheric oscillation parameters : Δm^2_{ATM}, θ_{ATM}. The best fit values for these parameter are today given by combining the results of SuperK with the ones from modern neutrino telescopes ANTARES and IceCube (Fig. 1.10). The other possibility is to measure these parameters in Long Baseline accelerator experiments.

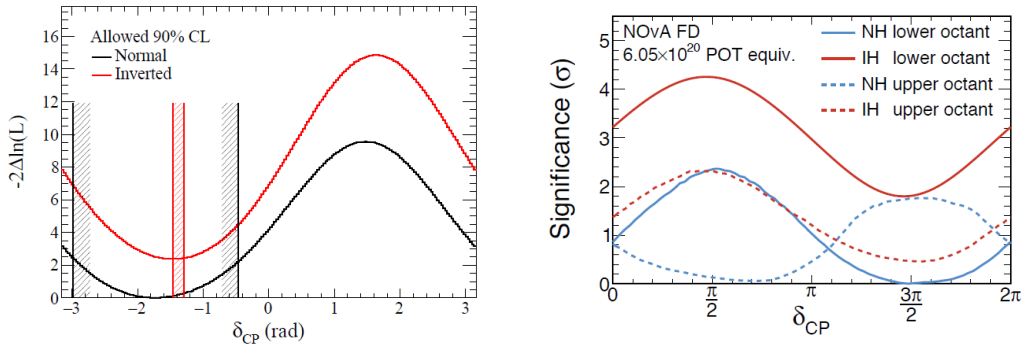

Figure 1.11: (Left) Log-likelihood function of $\delta_C P$ with 90% CL for normal (black) and inverted (red) hyerarchy at T2K (Right) Significance as function of $\delta_C P$ at NOνA in all combinations of mass ordering and $\theta_2 3$ octant

1.4.4 δ_{CP} experimental results

As already mention in Section most experiments that want to perform measurements of the CP phase are long baseline experiments with ν_μ and $\bar{\nu}_\mu$ accelerator beams with energy from $0.7GeV$ up to a few GeV. Specifically the CP asymmetries are usually measured as:

$$\mathcal{A}_{CP} = \frac{P(\nu_\mu \to \nu_e) - P(\bar{\nu}_\mu \to \bar{\nu}_e)}{P(\nu_\mu \to \nu_e) + P(\bar{\nu}_\mu \to \bar{\nu}_e)} \tag{1.48}$$

This observable can be approximated in the three-flavour case as:

$$\mathcal{A}_{CP} \simeq \frac{\cos\theta_{23} \sin 2\theta_{12}}{\sin\theta_{23} \sin\theta_{13}} \left(\frac{\Delta m^2_{21} L}{4E_\nu}\right) \sin\delta_{CP} + \text{matter effects} \tag{1.49}$$

It is clear then that if δ_{CP} is different from $0°$ and $\pm 180°$ one should expect to observe CP violation in the leptonic sector and $\mathcal{A}_{CP}$ would be different from 0 (i.e. $P(\nu_\mu \to \nu_e) \neq P(\bar{\nu}_\mu \to \bar{\nu}_e)$).
The latest measurements of δ_{CP} are from T2K. The experiment measured both the ν_μ survival probability and the ν_e appearence probability and then did the same for $\bar{\nu}_\mu$. The analysis excludes $\delta_C P = 0°, \pm 180°$ at 90% CL for both mass orderings.
Similar measurements have been performed by the NOνA experiment. The analysis found two best-fit points for normal mass ordering : $\sin^2\theta_{23} = 0.404$ $\delta_{CP} = 1.48\pi$ and $\sin^2\theta_{23} = 0.623$ $\delta_{CP} = 0.74\pi$. It also found that the inverted mass hordering is disfavoured at $> 93\%$ regardless of the value of the CP phase.

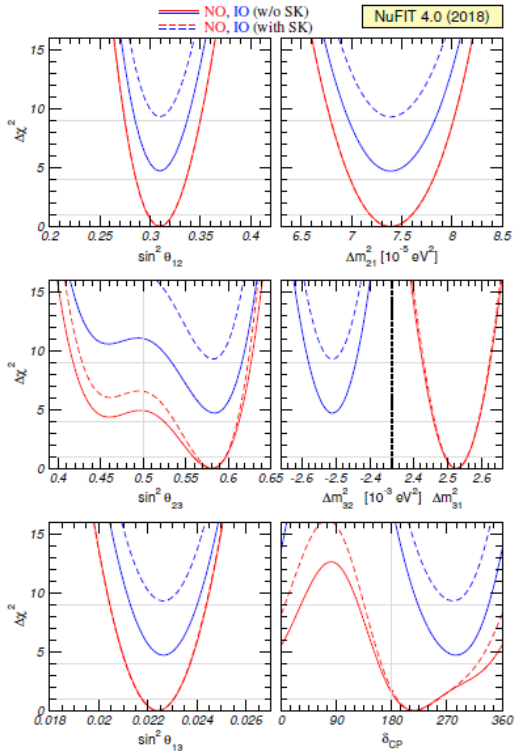

Figure 1.12: $\Delta\chi^2$ profile obtained from global 3ν oscillation experiments analysis. The profiles are minimized in all non displayed parameters. The red and and blue full curves correspond to the analysis resuts for NO and IO respectively, without considering the atmospheric data from SuperK. The dashed lines are with the inclusion of this data. For atmospheric mass squared difference Δm^2_{31} is used for NO and Δm^2_{32} for IO.

1.4.5 Mass hierarchy experimental results

As already mentioned in Section, thanks to matter effects it is possible to study mass ordering in long baseline experiments by appearence measurements, typically ν_e appearence in ν_μ beams. The most recent global fits performed on the oscillation parameters Δm^2_{32}, Δm^2_{31}, δ_{CP} and $\sin^2\theta_{23}$ from LBL accelerator experiments (NOνA, MINOS, T2K), reactor experiments (Data Bay, RENO, Double Chooz) and solar experiments (SNO, SuperK, Borexino) show a growing preference towards standard hierarchy. In particular the best fit can be obtained for NO while for IO one finds a $\Delta\chi^2 = 4.7$ (Fig. 1.12). The indication becomes even stronger when one includes data from the measurements on atmosferic neutrinos for SuperK where the value for IO becomes $\Delta\chi = 9.3$.

Parameter	Ordering	Best fit	1σ range	2σ range	3σ range
$\delta m^2/10^{-5}$ eV^2	NO, IO, Any	7.37	7.21 – 7.54	7.07 – 7.73	6.93 – 7.96
$\sin^2\theta_{12}/10^{-1}$	NO, IO, Any	2.97	2.81 – 3.14	2.65 – 3.34	2.50 – 3.54
$\lvert\Delta m^2\rvert/10^{-3}$ eV^2	NO	2.525	2.495 – 2.567	2.454 – 2.606	2.411 – 2.646
	IO	2.505	2.473 – 2.539	2.430 – 2.582	2.390 – 2.624
	Any	2.525	2.495 – 2.567	2.454 – 2.606	2.411 – 2.646
$\sin^2\theta_{13}/10^{-2}$	NO	2.15	2.08 – 2.22	1.99 – 2.31	1.90 – 2.40
	IO	2.16	2.07 – 2.24	1.98 – 2.33	1.90 – 2.42
	Any	2.15	2.08 – 2.22	1.99 – 2.31	1.90 – 2.40
$\sin^2\theta_{23}/10^{-1}$	NO	4.25	4.10 – 4.46	3.95 – 4.70	3.81 – 6.15
	IO	5.89	4.17 – 4.48 $\oplus$ 5.67 – 6.05	3.99 – 4.83 $\oplus$ 5.33 – 6.21	3.84 – 6.36
	Any	4.25	4.10 – 4.46	3.95 – 4.70 $\oplus$ 5.75 – 6.00	3.81 – 6.26
δ/π	NO	1.38	1.18 – 1.61	1.00 – 1.90	0 – 0.17 $\oplus$ 0.76 – 2
	IO	1.31	1.12 – 1.62	0.92 – 1.88	0 – 0.15 $\oplus$ 0.69 – 2
	Any	1.38	1.18 – 1.61	1.00 – 1.90	0 – 0.17 $\oplus$ 0.76 – 2

Figure 1.13: *
Results of recent 3ν oscillation global fits. The results are given in terms of best fit and $n\sigma$ ranges under the IO, NO and any ordering assumptions. Note that here $\delta m^2 \equiv \Delta m^2_{12}$, $\Delta m^2 = m^2_3 - (m^2_1 + m^2_2)/2$ and $\delta \equiv \delta_{CP}$ is given in terms of cycle intervals $\delta/\pi \in [0, 2]$.

1.5 Sate of the art and future prospects

Neutrino physics is entering its precision era with global fits restricting more and and more on the oscillation parameters values (Fig. 1.13). As outlined in the previous sections though there are still foundamental questions that are yet to be fully unswered :

- The determination of the absolute mass of the neutrinos and its origin i.e Majorana or Dirac;
- The measurement of CP asymmetries in the leptonic field;
- The determination of the mass ordering (normal or inverse)

While the first field of reaserch is in the domain of the types of experiments described in Section and, the latter two are best studied in oscillation experiments. Such goals will require levels of precision still not achieved and new experiments in all cathegories (reactor, atmospheric, ecc.).
In the long-baseline accelerator field DUNE (Deep Underground Neutrino Experiment), will be the next-generation flagship neutrino osclillation experiment of the Fermilab national laboratories. Having access to MSW effects and to a neutrino beam capable of producing both ν_μ and $\bar{\nu}_\mu$ will make it particularly well suited to probe mass hierarchy and CP violations respectively. This will be discussed more in detail in Chapter 2.

Bibliography

[1] Primo oggetto bibliografia.

[2] Secondo oggetto bibliografia.

[3] Terzo oggetto bibliografia.

[4] Quarto oggetto bibliografia.